



Article

Silver Nanoparticle/Carbon Nanotube Hybrid Nanocomposites: One-Step Green Synthesis, Properties, and Applications

Jun Natsuki¹ and Toshiaki Natsuki^{1,2,*}

¹ Institute for Fiber Engineering (IFES), Interdisciplinary Cluster for Cutting Edge Research (ICCER), Shinshu University, 3-15-1 Tokida, Ueda, Nagano 386 8567, Japan; jnatsu@shinshu-u.ac.jp

² Faculty of Textile Science and Technology, Shinshu University, 3 15 1 Tokida, Ueda shi, Nagano 386 8567, Japan

* Correspondence: natsuki@shinshu-u.ac.jp

Abstract: Hybrid nanocomposites of silver nanoparticles and multiwalled carbon nanotubes (Ag-NPs/MWCNTs) were successfully synthesized by a green one-step method without using any organic solvent. The synthesis and attachment of AgNPs onto the surface of MWCNTs were performed simultaneously by chemical reduction. In addition to their synthesis, the sintering of AgNPs/MWCNTs can be carried out at room temperature. The proposed fabrication process is rapid, cost efficient, and ecofriendly compared with multistep conventional approaches. The prepared AgNPs/MWCNTs were characterized using transmission electron microscopy (TEM) and X-ray photoelectron spectroscopy (XPS). The transmittance and electrical properties of the transparent conductive films (TCF_Ag/CNT) fabricated using the prepared AgNPs/MWCNTs were characterized. The results showed that the TCF_Ag/CNT film has excellent properties, such as high flexible strength, good high transparency, and high conductivity, and could therefore be an effective substitute for conventional indium tin oxide (ITO) films with poor flexibility.

Keywords: silver nanoparticles; carbon nanotubes; synthesis; green one-step method



Citation: Natsuki, J.; Natsuki, T. Silver Nanoparticle/Carbon Nanotube Hybrid Nanocomposites: One-Step Green Synthesis, Properties, and Applications. *Nanomaterials* **2023**, *13*, 1297. <https://doi.org/10.3390/nano13081297>

Academic Editors: Alexey Pestryakov and Rosario Pereiro

Received: 8 March 2023

Revised: 5 April 2023

Accepted: 5 April 2023

Published: 7 April 2023



Copyright: © 2023 by the authors. Licensee MDPI, Basel, Switzerland. This article is an open access article distributed under the terms and conditions of the Creative Commons Attribution (CC BY) license (<https://creativecommons.org/licenses/by/4.0/>).

1. Introduction

High electrical conductivity and high optical transparency are desired for transparent conductive films (TCFs). Commonly used TCFs, such as indium tin oxide (ITO) film, have been widely applied to touch screen, panel display, liquid crystal displays, and solar cells [1–3]. However, ITO films are high cost owing to the lack of indium source. In addition, the resistance of ITO thin films increases remarkably with bending force. The brittleness of ITO has limited its applications in flexible electronic devices owing to the low bending strength and particle size of indium [4,5]. Thus, ITO films must be replaced with cost effective and high-performance flexible materials. **Alternative materials, such as carbon nanotubes** (CNTs) decorated with silver nanoparticles (AgNPs), have been studied for their synthesis **and electricity** evaluation. CNTs, which are cylinder-shaped allotropic forms of carbon, exhibit interesting mechanical and physical properties, such as high strength, unique electronic state, and efficient heat conductivity and optical transmission [6–9]. CNTs have novel properties that make them suitable in many applications, including engineering, nanotechnology, and materials science [10–13].

The **synthesis** of AgNPs has received remarkable attention in the field of materials science [14–17]. AgNPs are widely used in the electronics industry for printed electronic circuits due to their advantages, such as high electrical conductivity and nanometer scale [18–21]. However, the fragility of AgNPs results in the lack of flexibility of the film prepared from this material. Given the individual benefits of CNTs and AgNPs, their composites can reach highly effective materials that cannot be achieved independently [22].

Many works have described fabrication processes for flexible TCFs using CNTs [23–29]. Transparent CNT film production mainly includes drop-drying from solvent, airbrushing,

and Langmuir–Blodgett deposition. An early work by Geng et al. [24] reported a relatively straightforward approach to fabricate large-sized TCFs using single-walled CNTs (SWCNTs) by spray coating using sodium dodecyl sulfate (SDS)-dispersed SWCNTs. A comprehensive review was conducted on CNT TCFs and detailed fabrication methods, such as film patterning, chemical doping effects, and hybridization with other materials [25]. The review also focused on the optoelectronic properties of the films and their potential applications of photovoltaics, touch panels, and liquid crystal displays. Zhou and Azumi [27] reviewed and summarized the recent progress in the fabrication, properties, and application of CNT-based TCFs to open new opportunities in the development of next-generation flexible displays. They also gave some possible strategies to reduce the production cost and improve the conductivity and transparency. Hou et al. [28] obtained high-quality double-walled CNT-based TCFs fabricated by scalable filtration and showing extremely low sheet resistance of $83 \Omega/\text{sq}$ with transmittance of 79% at 550 nm.

AgNPs are well known for their high electrical conductivity and antimicrobial properties. Adding AgNPs can effectively improve the electrical conductivity of nanocomposites and provide good antibacterial properties compared with pristine CNTs. Some studies were conducted on various CNT films decorated with various AgNP concentrations [30–35]. Yu et al. [31] used a potentiostatic double-pulse technique to electrodeposit AgNPs onto multiwalled CNT (MWCNTs) multilayer films preassembled on ITO. The results showed that AgNPs of 10–500 nm with varied density could be electrogenerated on MWCNT surface, and the MWCNT electrodes exhibited good conductivity. Lin et al. [32] developed a novel nonenzymatic sensor with high sensitivity using polydopamine (PDA) as a multifunctional intermediate for depositing AgNPs onto SWCNTs. The advantages of the sensor could be ascribed to using CNTs and AgNPs. Due to the large surface area, CNTs were used as an effective matrix for AgNP loading due to the large surface area to improve the conductivity of the nanocomposite, and AgNPs were attached to SWCNTs through in situ chemical reduction by PDA to improve the surface active for electrochemical catalysis. Shi et al. [35] reported that cetylpyridinium borohydride (CBH4)-coated MWCNT could be used as a template for the synthesis of AgNPs on MWCNTs. The obtained AgNP/MWCNT hybrid material showed a promising electrocatalytic performance. Although these studies explored synthesis procedures for hybrid nanostructures consisting of CNTs and AgNPs using chemical reaction methods, only a few reports focused on CNT-based nanocomposites decorated with AgNPs for preparing high-performance TCFs [36–38]. Lee et al. [36] prepared TCFs fabricated with DWNT-AgNP suspension using a wet coating method. The prepared DWNT-AgNP thin films had a low sheet resistance of $53.4 \Omega/\text{sq}$ and an optical transmittance of 90.5%. Ko et al. [37] showed that the sheet resistance remained approximately $370 \Omega/\text{sq}$, even after 500 bending cycles, with a transmittance of around 77%. Li et al. [38] achieved optoelectronic properties with sheet resistance of $50.3 \Omega/\text{sq}$ and a high transmittance of 79.73% at a wavelength of 550 nm.

In this work, we proposed a one-step green method to decorate AgNPs on the surface of MWCNTs. Organic solvent was not used, and the reaction proceeded at room temperature. AgNP/MWCNT nanocomposites with uniform, 5 nm diameter AgNPs on the surface of MWCNTs were effectively obtained by simple separation. The developed method is suitable for practical applications because it is an easy and environmentally benign process. Furthermore, electronic circuits prepared with the AgNP/MWCNT nanocomposites can be manufactured easily by sintering at low temperature because no dispersing polymer was used. The transmittance and electrical properties of the TCF_Ag/CNT film fabricated using the AgNP/MWCNT nanocomposites were also characterized. The results showed that the TCF_Ag/CNT film has excellent properties, such as high flexible strength, good transparency, and high conductivity.

2. Experimental Section

2.1. Materials

Sodium gluconate, sodium citrate (Na_3Ct), silver nitrate (AgNO_3), and dimethylaminoethanol (DMAE; 2-dimethylaminoethanol) were purchased from Wako Inc., Japan. Nitric acid (HNO_3) and lysine (L(+)-Lysine) (Wako, Inc., Tokyo, Japan) were used as solvents. Gallic acid (gallic acid monohydrate) was obtained from Wako, Japan. Deionized water was used throughout the experiments.

2.2. Preparation of Functionalized MWCNTs

MWCNTs ($d = 20\text{--}30$ nm, Wako Inc., Tokyo, Japan) were used in this study. CNTs have high physical durability, lightweight, flexibility, and excellent electrical and thermal conductivity. CNTs exhibit low reactivity because they lack functional groups. For easy dispersion and bonding of AgNPs onto the CNT surfaces, the CNTs were modified to introduce functional groups onto their surfaces. The functional group introduced onto the CNTs was not particularly limited, forming a hydrogen bond (intermolecular force bond) with a hydroxyl group ($-\text{OH}$) or a carboxylic acid ($-\text{COOH}$) group. In this work, two kinds of methods using nitric acid (HNO_3) and lysine (L(+)-Lysine) were used to modify the MWCNTs.

Nitric acid-modified MWCNTs were obtained through the following steps. First, 0.15 g of MWCNTs and 70 mL of HNO_3 were placed in a flask and stirred at 120°C for 10 h in an oil bath. The obtained reaction solution was then centrifuged at $5000\times g$ rpm for 1 min, and the supernatant was discarded. The precipitate was washed with pure water and centrifuged twice at 5000 rpm for 2 min. The modified CNTs were placed in 1 L of pure water and left for 24 h to neutralize their pH. After centrifugation at 5000 rpm for 1 min, the supernatant was discarded, and the residue was dried at 60°C for 24 h to obtain nitric acid-modified MWCNTs.

Lysine-modified MWCNTs were obtained as follows. In brief, 0.25 g of lysine was stirred in a beaker with 120 mL of purified water at 60°C until completely dissolved. The solution was then added with 0.25 g of MWCNTs, stirred at 60°C for 2 h, and centrifuged at 5000 rpm for 1 min. The supernatant was discarded, and the precipitate was washed with pure water and centrifuged twice at $5000\times g$ rpm for 2 min. The modified CNTs were placed in 1 L of pure water and left for 24 h to neutralize their pH. After centrifugation at 5000 rpm for 1 min, the supernatant was discarded and dried at 60°C for 24 h to obtain lysine-modified MWCNTs.

When nitric acid is used for the surface treatment of MWCNTs, the procedure must be conducted at high temperature for a long time. The method also requires time and effort to make the sample neutral because a strong acid is used. Therefore, we developed a simple treatment method that uses lysine and has the merit of processing at a low temperature and in a short period of time.

2.3. Fabrication of AgNP/MWCNT Nanocomposites

A simple, green one-step synthesis method was developed to synthesize AgNP/MWCNT nanocomposites. Figure 1 shows the fabrication of AgNPs/MWCNTs in which MWCNTs were used as a dispersing agent. All the above steps were performed at room temperature.

In brief, 0.04 g of the modified MWCNTs (Section 2.2) were added to 20 mL of pure water and stirred at room temperature for 10 min. The solution was then added with 0.5 g of silver nitrate and stirred for another 10 min, followed by the addition of an aqueous solution of gallic acid dissolved in 30 mL of pure water and 0.262 g of DMAE, stirring for 1 h. The obtained reaction solution was centrifuged at 5000 rpm for 1 min, the supernatant was discarded, and the precipitate was washed with pure water. After the steps were repeated twice (centrifugation at 5000 rpm for 2 min), the precipitate was redispersed in 10 mL of ethanol to obtain an aqueous dispersion of AgNP/MWCNT nanocomposites. For the preparation of pure AgNPs/MWCNTs, the resulting product was centrifuged, washed with pure water, and dried overnight at 60°C .

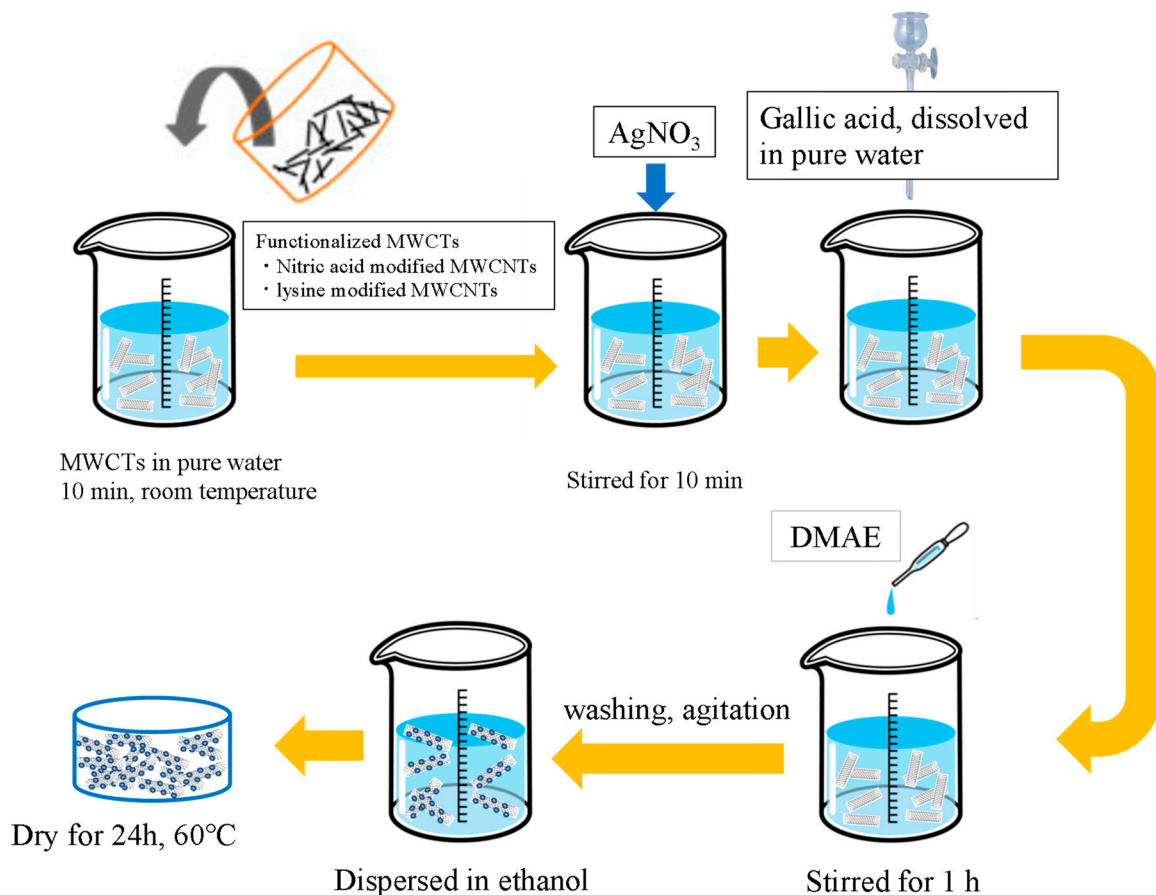


Figure 1. Fabrication process of AgNP/MWCNT nanocomposites.

2.4. Preparation of AgNP/MWCNT Film (TCF_Ag/CNT)

Polyethylene terephthalate (PET, U34, 100 μm , Co., Ltd., Toyama, Japan) film was used as the substrate of the TCFs. The PET films were cleaned using an ultrasonic cleaner **with ethanol** for about 10 s to remove surface debris, washed with pure water, and dried. TCF_Ag/CNT was prepared by coating the PET surface with AgNPs/MWCNTs.

The coating method was as follows: AgNPs/MWCNTs were dispersed in isopropyl alcohol (IPA, Wako Inc., Tokyo, Japan). The PET substrate was placed on a hot plate at a temperature of 60°C . With the spray method, TCF_Ag/CNT was coated at 15 cm distance between the substrate and spray nozzle as shown in Figure 2. TCF_Ag/CNT was fabricated using two types of modified CNT: nitric acid-modified (CNT_HNO₃) and lysine-modified (CNT_lyine). TCF_Ag/CNT films were prepared using 0.001, 0.005, and 0.01 g of AgNPs/MWCNTs under nitric acid modification and denoted as TCF_Ag/CNT_HNO₃ 0.001 g, TCF_Ag/CNT_HNO₃ 0.005 g, and TCF_Ag/CNT_HNO₃ 0.01 g, respectively. With the same method, TCF_Ag/CNT_lyine 0.001 g, TCF_Ag/CNT_lyine 0.005 g, and TCF_Ag/CNT_lyine 0.01 g were fabricated using the lysine-modified AgNPs/MWCNTs. The thickness of coating layer affects the light transmittance. The transmittance decreases with increasing film thickness. In order to obtain transmittance, the film thicknesses of all the samples are less than 1 μm in this work.

2.5. Characterization Methods

The AgNP/MWCNT nanocomposites were characterized using various measurements including UV-Vis spectroscopy (Hitachi U-4100 UV-Vis Spectrophotometer), X-ray diffraction (XRD) (Rigaku D/MAX-III X-ray Diffractometer with Cu-K α radiation), transmission electron microscopy (TEM, JEOL JEM2010 operating at 200 kV), energy dispersive X-ray spectroscopy (EDS) (FE-SEM, Hitachi S-5000 equipped with an EDS instrument), and

X-ray photoelectron spectroscopy (XPS) (Kratos Axis Ultra DLD, Kratos Analytical Ltd., Manchester, UK). The electrical properties of samples were measured using a resistivity meter (Loresta-GP, MCP-T700, Mitsubishi Chemical Ltd., Tokyo, Japan).

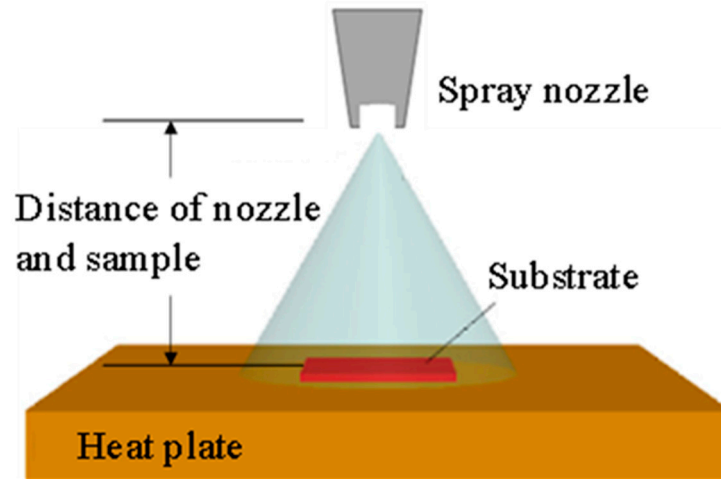


Figure 2. Schematic of spray coating deposition for thin film.

3. Results and Discussion

3.1. Characterization of AgNPs/MWCNTs

TEM and XPS analyses were used to characterize the functional groups on the surfaces of MWCNTs and AgNP/MWCNT nanocomposites. Figures 3 and 4 show the TEM images of AgNPs/MWCNTs nanocomposites. The AgNPs had a spherical shape and uniform diameter of about 5 nm and were homogeneously dispersed without agglomeration and strongly adhered to the surface of the MWCNTs. As shown in Figure 4, it was observed that the AgNPs are distributed uniformly on the CNT's surface with high ratio in the nanocomposites, having a diameter of 20–30 nm. This phenomenon was attributed to the condensation reaction between the functional groups on the CNT surfaces and AgNPs, resulting in the AgNPs adhering to the CNTs without aggregation. The reduced AgNPs are covered with a reducing agent layer. Therefore, the AgNPs become very stable due to the strong binding of AgNPs with the functional groups introduced to the CNT surface through the covering layer.

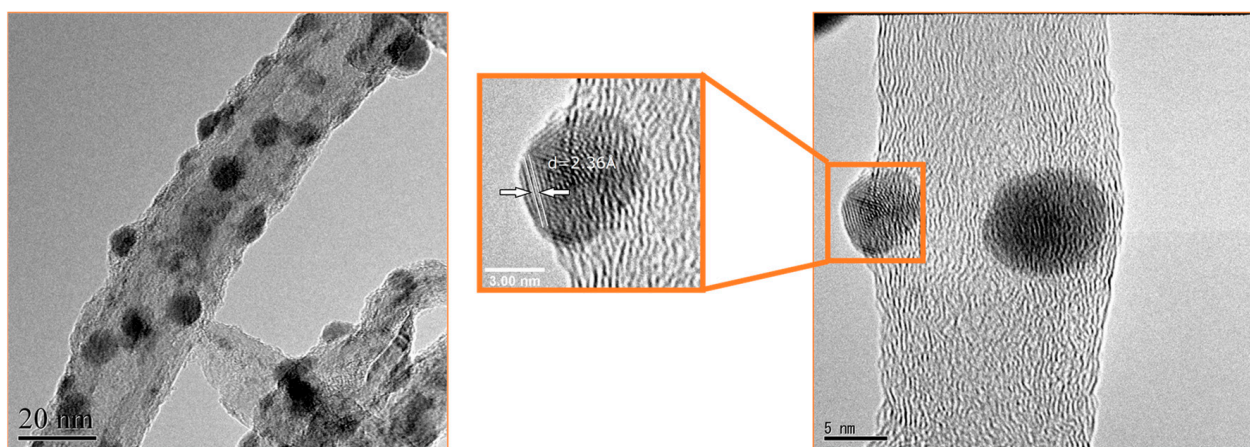


Figure 3. TEM micrographs of AgNP/MWCNT nanocomposites.

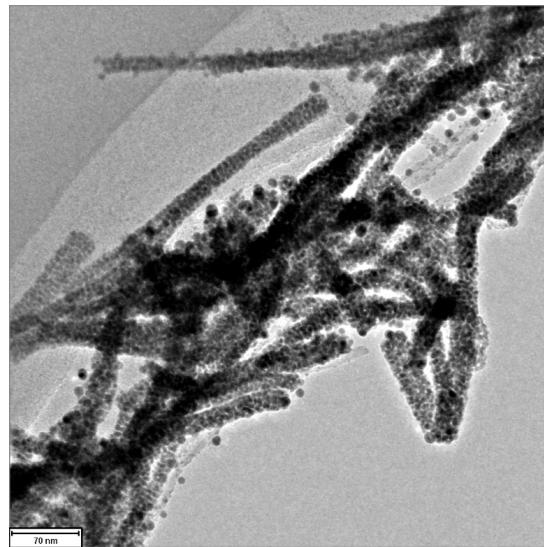


Figure 4. TEM micrograph of the distribution image of AgNPs attached on the CNTs.

Figure 5 shows the XPS survey spectra of modified MWCNTs, Ag/CNT_HNO₃, and Ag/CNT_lysine. The peak of C1s, Ag3d, and Ag3p confirmed the existence of carbon and the formation of AgNPs. C1s showed a strong peak at 284 eV and O1s at 532 eV. The Ag3p peaks composed of Ag3p3/2 and Ag3p1/2 contained two strong peaks at 573 and 604 eV. Furthermore, the amplified region around the Ag3d peaks is shown in Figure 6. The XPS survey spectrum of Ag3d was composed of Ag3d5/2 and Ag3d3/2, showing strong peaks at 368 and 374 eV, respectively. The difference between the Ag3d5/2 and Ag3d3/2 peaks was 6 eV, which proved the formation of crystalline AgNPs.

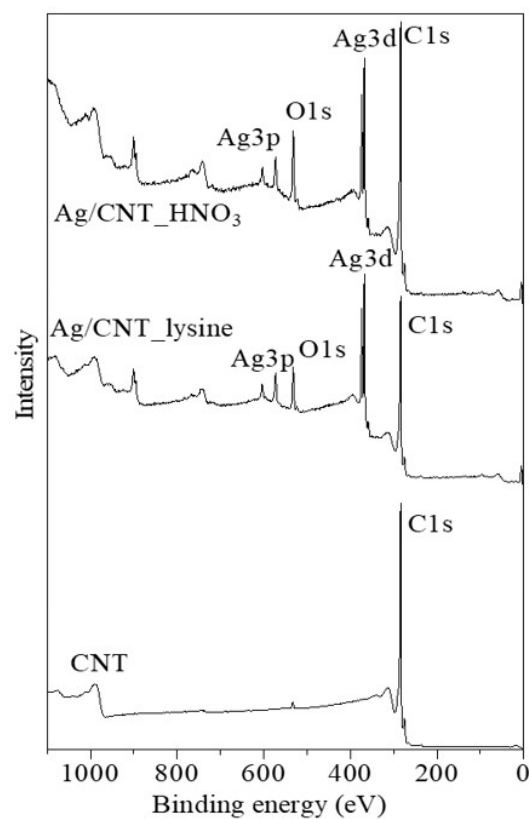


Figure 5. XPS survey spectrum of the AgNP/MWCNT nanocomposites.

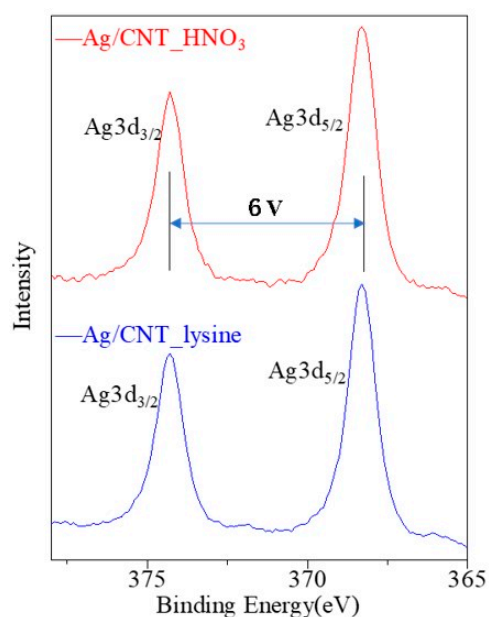


Figure 6. High-resolution XPS survey spectrum of the Ag3d peak.

3.2. Characterization of AgNP/MWCNT Films (TCF_Ag/CNT)

FE-SEM images and EDS analysis of TCF_Ag/CNT_HNO₃ and TCF_Ag/CNT_lysine are shown in Figure 7. The AgNPs adhered to the TCF's surface. The AgNP/MWCNT films contained AgNPs with high ratio and no impurities were found, as shown in the EDS analysis of Table 1.

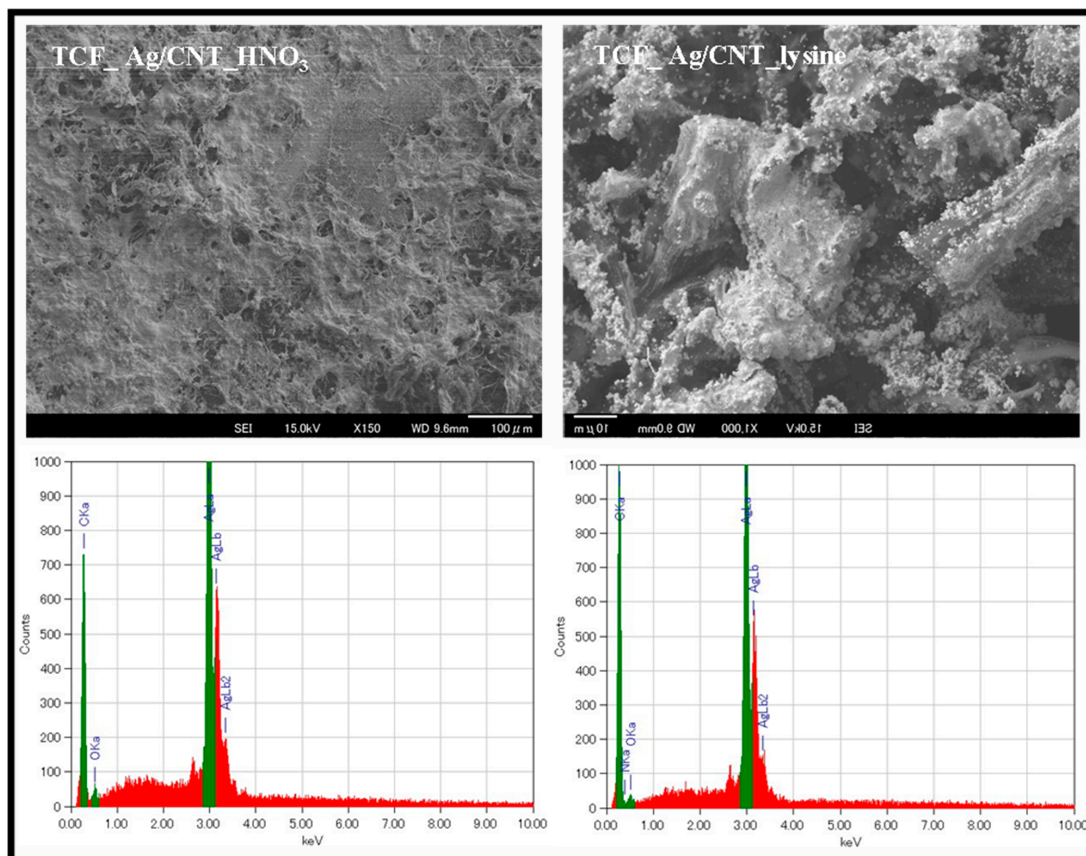


Figure 7. FE-SEM images and EDS analysis of AgNP/MWCNT nanocomposites.

Table 1. Ratio of Ag element (mass %) in TCF_Ag/CNT nanocomposites.

Samples	Ag
TCF_Ag/CNT_HNO ₃	84.6
TCF_Ag/CNT_lysine	76.7

3.3. Transmittance of AgNP/MWCNT Films

The relationship between the transmittance and wavelength waveform was measured for the TCF_Ag/CNT films prepared in Section 2.4. The transmittance at the visible wavelength of 550 nm was taken as the transmittance of the film. In this study, the transmittance of the substrate PET film is 100%, and the measured material is regarded as transparent when the transmittance of substrates exceeds 80%.

Figure 8 shows the variation of transmittance with the wavelength of TCF_Ag/CNT thin films with two different surface treatment methods. The TCF_Ag/CNT thin films fabricated using 0.01 g of AgNPs/MWCNTs had transmittances of 20.4% and 2.0% in the wavelength of 550 nm for TCF_Ag/CNT_lysine and TCF_Ag/CNT_HNO₃, respectively. The transmittance of TCF_Ag/CNT_lysine was 10 times as high as that of Ag/CNT_HNO₃. Figure 9 shows the relationship between the transmittance of TCF_Ag/CNT_lysine thin films and the wavelength under different amounts of added AgNPs/MWCNTs. The transmittance of TCF_Ag/CNT_lysine reached a high value of 89.7% in the wavelength of 550 nm when the amount of added AgNPs/MWCNTs was 0.001 g. The transmittance under the addition of 0.01 and 0.005 g of TCF_Ag/CNT_lysine was 59.1% and 20.4%, respectively. Therefore, films with high transmittance can be fabricated using AgNP/CNT_lysine nanocomposites.

3.4. Electrical Conductivity of AgNP/MWCNT Films

The electrical conductivity properties of the TCF_Ag/CNT films prepared in Section 2.4 were measured using Loresta-GP MCP-T610 resistivity meter (Mitsubishi Chemical Analytech Co., Ltd., Tokyo, Japan). Figure 10 shows the relationship between surface resistivity and transmittance for TCF_Ag/CNT_lysine and TCF_Ag/CNT_HNO₃. The electric resistance of TCF_Ag/CNT_lysine was lower than that of TCF_Ag/CNT_HNO₃, indicating that TCF can be successfully produced by the spray coating method. Moreover, we investigated the change in the electrical resistance of TCF_Ag/CNT_lysine before and after bending. The electrical resistance before bending was $22 \times 10^4 \Omega$, and the electrical resistance after bending was $35 \times 10^4 \Omega$. Almost no change of electrical resistance was observed before and after bending. The reason is that the MWCNTs have a high aspect ratio and superior mechanical and electrical properties. ITO is a good transparent conductive material applied to electronic devices. However, the ITO film has low flexible strength because of the sintered ITO particles with large size. In this study, the TCF film fabricated with AgNP/MWCNT nanocomposites is strong against bending due to the flexibility of CNTs. The TCF_Ag/CNT films have high mechanical flexibility, high transparency, and high conductivity, showing potential application to screen panels, thin film transistors, and field emission devices.

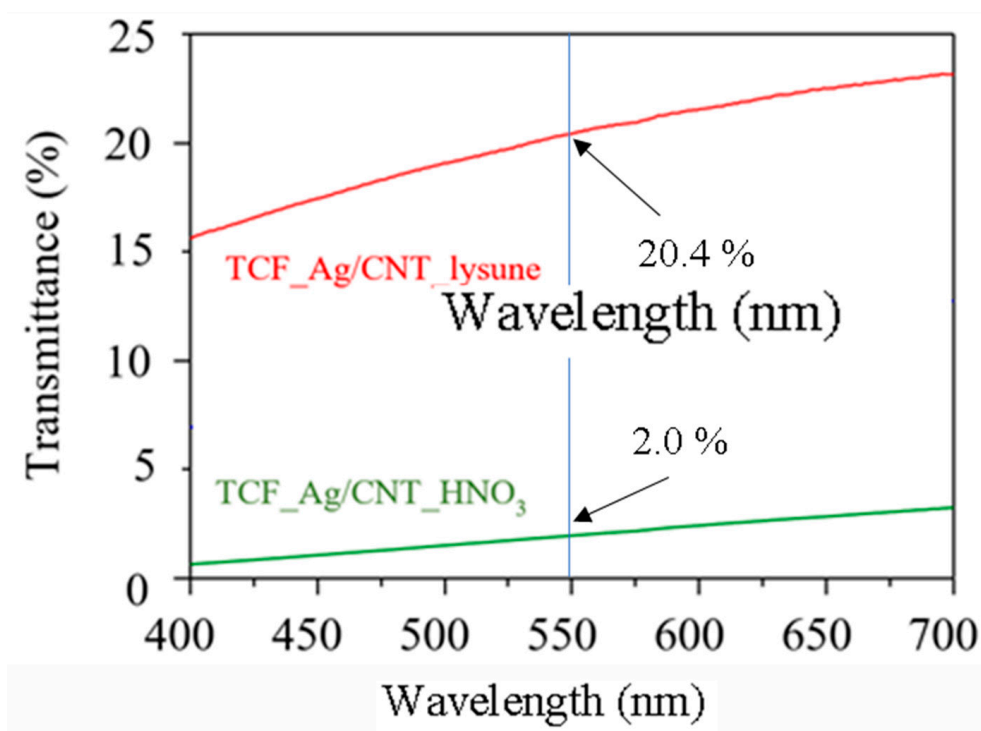


Figure 8. Variation of the optical transmittance of AgNP/MWCNT films with the wavelength.

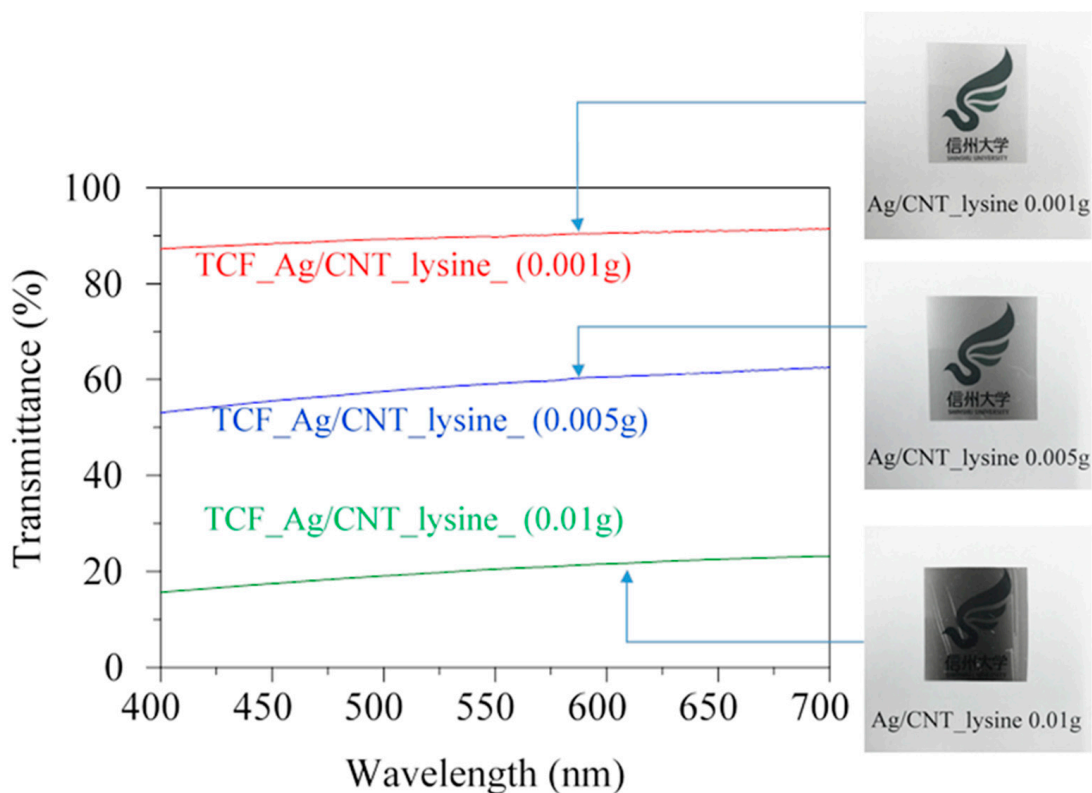


Figure 9. Relationship between the optical transmittance of AgNP/MWCNT films of different amounts and the wavelength.

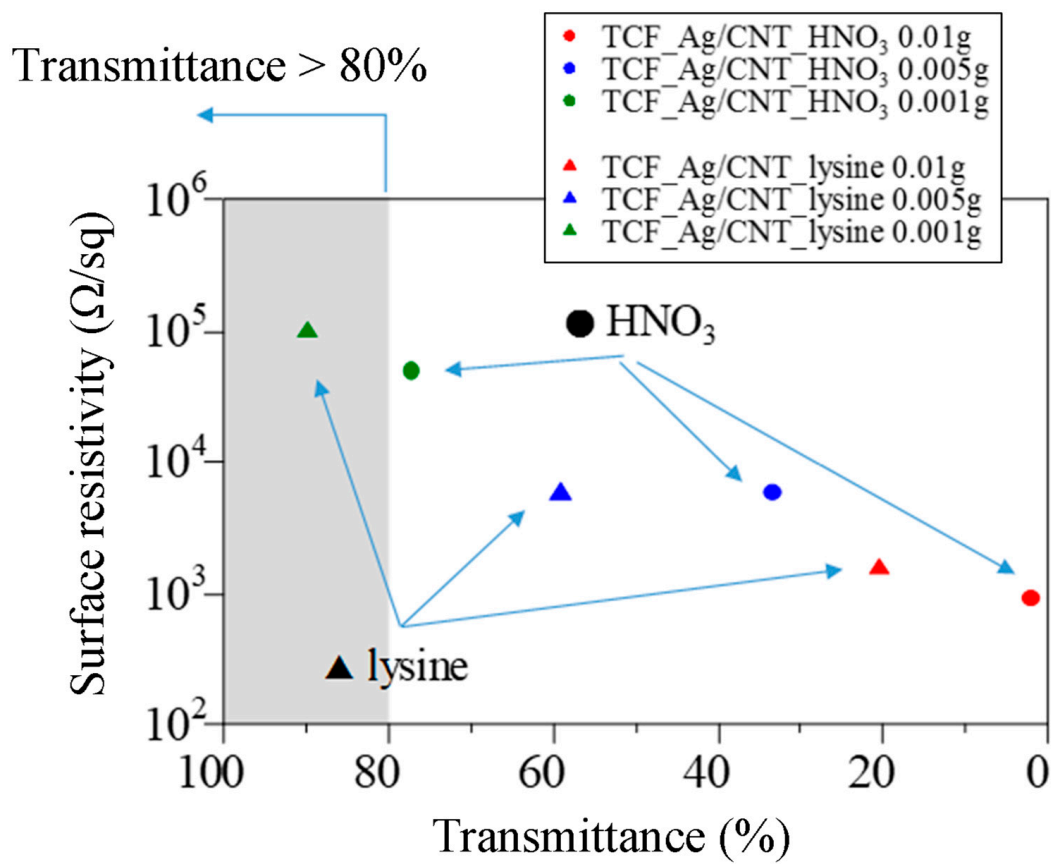


Figure 10. Relationship between the surface resistivity of AgNP/MWCNT films and the transmittance.

4. Conclusions

In this study, a simple, green one-step method was developed to synthesize AgNP/MWCNT nanocomposites. The synthesis and attachment of AgNPs onto the surface of MWCNTs were carried out simultaneously at room temperature without using any organic solvent. The AgNP/MWCNT nanocomposites are easily separated from solution because no organic solvent is used. Moreover, the TCF film fabricated with the AgNP/MWCNT nanocomposites can be sintered easily at a low temperature because no dispersing polymer was used in the fabrication. Taking advantage of the excellent properties of AgNPs and CNTs, the prepared TCF_Ag/CNT films have excellent properties, such as high flexible strength, good transparency, and high conductivity. These advantages render the TCF_Ag/CNT films an effective substitute for conventional ITO films with poor flexibility. Therefore, the developed method is suitable for practical applications because the manufacturing process has the advantage of environmental friendliness.

Author Contributions: J.N. Investigation, Methodology, All experiments and data analysis, Writing-original draft and review; T.N. Investigation, Supervision, Writing-review and editing. All authors have read and agreed to the published version of the manuscript.

Funding: This research received no external funding.

Institutional Review Board Statement: Not applicable.

Informed Consent Statement: Not applicable.

Data Availability Statement: Not applicable.

Conflicts of Interest: The authors declare no conflict of interest.

References

1. Seo, D.J.; Shim, J.P.; Choi, S.B.; Seo, T.H.; Suh, E.K.; Lee, D.S. Efficiency improvement in InGaN-based solar cells by indium tin oxide nano dots covered with ITO films. *Opt. Express* **2012**, *20*, A991–A996. [[CrossRef](#)] [[PubMed](#)]
2. Wang, S.; He, Y.; Yang, J.; Feng, Y. Enrichment of indium tin oxide from colour filter glass in waste liquid crystal display panels through flotation. *J. Clean. Prod.* **2018**, *189*, 464–471. [[CrossRef](#)]
3. Kim, J.; Kim, B.-K.; Park, K. Electrodeposition of Silver Nanoparticles on Indium-Doped Tin Oxide Using Hydrogel Electrolyte for Hydrogen Peroxide Sensing. *Nanomaterials* **2022**, *13*, 48. [[CrossRef](#)] [[PubMed](#)]
4. Alzoubi, K.; Hamasha, M.M.; Lu, S.; Sammakia, B. Bending Fatigue Study of Sputtered ITO on Flexible Substrate. *J. Disp. Technol.* **2011**, *7*, 593–600. [[CrossRef](#)]
5. Rathore, S.; Singh, A. Bending fatigue damage reduction in indium tin oxide (ITO) by polyimide and ethylene vinyl acetate encapsulation for flexible solar cells. *Eng. Res. Express* **2020**, *2*, 015022. [[CrossRef](#)]
6. Xie, S.; Li, W.; Pan, Z.; Chang, B.; Sun, L. Mechanical and physical properties on carbon nanotube. *J. Phys. Chem. Solids* **2000**, *61*, 1153–1158. [[CrossRef](#)]
7. Yu, M.-F.; Lourie, O.; Dyer, M.J.; Moloni, K.; Kelly, T.F.; Ruoff, R.S. Strength and Breaking Mechanism of Multiwalled Carbon Nanotubes Under Tensile Load. *Science* **2000**, *287*, 637–640. [[CrossRef](#)]
8. Volkov, A.N.; Zhitomirsky, L.V. Heat conduction in carbon nanotube materials: Strong effect of intrinsic thermal conductivity of carbon nanotubes. *Appl. Phys. Lett.* **2012**, *101*, 043113. [[CrossRef](#)]
9. Goupalov, S.V. Optical transitions in carbon nanotubes. *Phys. Rev. B* **2005**, *72*, 195403. [[CrossRef](#)]
10. Pei, B.; Wang, W.; Dunne, N.; Li, X. Applications of Carbon Nanotubes in Bone Tissue Regeneration and Engineering: Superiority, Concerns, Current Advancements, and Prospects. *Nanomaterials* **2019**, *9*, 1501. [[CrossRef](#)]
11. Saito, N.; Usui, Y.; Aoki, K.; Narita, N.; Shimizu, M.; Hara, K.; Ogiwara, N.; Nakamura, K.; Ishigaki, N.; Kato, H.; et al. Carbon nanotubes: Biomaterial applications. *Chem. Soc. Rev.* **2009**, *38*, 1897–1903. [[CrossRef](#)]
12. Inganäs, O.; Lundström, I. Materials science—Carbon nanotube muscles. *Science* **1999**, *284*, 1281–1282. [[CrossRef](#)]
13. Shi, K.; Zhitomirsky, I. Electrophoretic nanotechnology of graphene–carbon nanotube and graphene–polypyrrole nanofiber composites for electrochemical supercapacitors. *J. Colloid Interface Sci.* **2013**, *407*, 474–481. [[CrossRef](#)] [[PubMed](#)]
14. Salkar, R.A.; Jeevanandam, P.; Aruna, S.T.; Koltypin, Y.; Gedanken, A. The sonochemical preparation of amorphous silver nanoparticles. *J. Mater. Chem.* **1999**, *9*, 1333–1335. [[CrossRef](#)]
15. Natsuki, J.; Abe, T. Synthesis of pure colloidal silver nanoparticles with high electroconductivity for printed electronic circuits: The effect of amines on their formation in aqueous media. *J. Colloid Interface Sci.* **2011**, *359*, 19–23. [[CrossRef](#)]
16. Sampath, G.; Chen, Y.-Y.; Rameshkumar, N.; Krishnan, M.; Nagarajan, K.; Shyu, D.J.H. Biologically Synthesized Silver Nanoparticles and Their Diverse Applications. *Nanomaterials* **2022**, *12*, 3126. [[CrossRef](#)] [[PubMed](#)]
17. Wang, H.; Qiao, X.; Chen, J.; Wang, X.; Ding, S. Mechanisms of PVP in the preparation of silver nanoparticles. *Mater. Chem. Phys.* **2005**, *94*, 449–453. [[CrossRef](#)]
18. Htwe, Y.; Abdullah, M.; Mariatti, M. Water-based graphene/AgNPs hybrid conductive inks for flexible electronic applications. *J. Mater. Res. Technol.* **2022**, *16*, 59–73. [[CrossRef](#)]
19. Bhujel, R.; Swain, B.P. Investigation of electronic environments and electrical characterization of functionalised AgNPs synthesized by electroless process. *Appl. Phys. A* **2019**, *125*, 565. [[CrossRef](#)]
20. Magdassi, S.; Bassa, A.; Vinetsky, Y.; Kamyshny, A. Silver Nanoparticles as Pigments for Water-Based Ink-Jet Inks. *Chem. Mater.* **2003**, *15*, 2208–2217. [[CrossRef](#)]
21. Ivanisevi, I.; Kovaci, M.; Zubak, M.; Ressler, A.; Krivaci, S.; Katanci, Z.; Pavlovic, I.G.; Kassal, P. Amphiphilic silver nanoparticles for inkjet-printable conductive inks. *Nanomaterials* **2022**, *12*, 4252. [[CrossRef](#)]
22. Fortunati, E.; D’Angelo, F.; Martino, S.; Orlacchio, A.; Kenny, J.; Armentano, I. Carbon nanotubes and silver nanoparticles for multifunctional conductive biopolymer composites. *Carbon* **2011**, *49*, 2370–2379. [[CrossRef](#)]
23. Wu, Z.; Chen, Z.; Du, X.; Logan, J.M.; Sippel, J.; Nikolou, M.; Kamaras, K.; Reynolds, J.R.; Tanner, D.B.; Hebard, A.F.; et al. Transparent, Conductive Carbon Nanotube Films. *Science* **2004**, *305*, 1273–1276. [[CrossRef](#)]
24. Geng, H.-Z.; Kim, K.K.; So, K.P.; Lee, Y.S.; Chang, Y.; Lee, Y.H. Effect of Acid Treatment on Carbon Nanotube-Based Flexible Transparent Conducting Films. *J. Am. Chem. Soc.* **2007**, *129*, 7758–7759. [[CrossRef](#)]
25. Yu, L.; Shearer, C.; Shapter, J. Recent Development of Carbon Nanotube Transparent Conductive Films. *Chem. Rev.* **2016**, *116*, 13413–13453. [[CrossRef](#)] [[PubMed](#)]
26. Jiang, S.; Hou, P.-X.; Liu, C.; Cheng, H.-M. High-performance single-wall carbon nanotube transparent conductive films. *J. Mater. Sci. Technol.* **2019**, *35*, 2447–2462. [[CrossRef](#)]
27. Zhou, Y.; Azumi, R. Carbon nanotube based transparent conductive films: Progress, challenges, and perspectives. *Sci. Technol. Adv. Mater.* **2016**, *17*, 493–516. [[CrossRef](#)] [[PubMed](#)]
28. Hou, P.-X.; Yu, B.; Su, Y.; Shi, C.; Zhang, L.-L.; Liu, C.; Li, S.; Du, J.-H.; Cheng, H.-M. Double-wall carbon nanotube transparent conductive films with excellent performance. *J. Mater. Chem. A* **2013**, *2*, 1159–1164. [[CrossRef](#)]
29. Fraser, I.S.; Motta, M.S.; Schmidt, R.K.; Windle, A.H. Continuous production of flexible carbon nanotube-based transparent conductive films. *Sci. Technol. Adv. Mater.* **2010**, *11*, 045004. [[CrossRef](#)]
30. Taqwa, Y.Y.; Asama, N.N. Characterization of carbon nanotube decorated silver nanoparticles. *J. Phys. Conf. Ser.* **2021**, *1879*, 032093.

31. Yu, A.; Wang, Q.; Yong, J.; Mahon, P.J.; Malherbe, F.; Wang, F.; Zhang, H.; Wang, J. Silver nanoparticle–carbon nanotube hybrid films: Preparation and electrochemical sensing. *Electrochim. Acta* **2012**, *74*, 111–116. [[CrossRef](#)]
32. Lin, Y.; Li, L.; Hu, L.; Liu, K.; Xu, Y. Multifunctional poly(dopamine)-assisted synthesis of silver nano particles/carbon nanotubes nanocomposite: Toward electrochemical sensing of hydrogen peroxide with enhanced sensitivity. *Sens. Actuators B Chem.* **2014**, *202*, 527–535. [[CrossRef](#)]
33. Amaku, J.F.; Martincigh, B.S. Synthesis and Characterization of Nanocomposites Containing Silver Nanoparticle—Decorated Multiwalled Carbon Nanotubes for Water Disinfection. *Waste Biomass-Valorization* **2021**, *13*, 149–172. [[CrossRef](#)]
34. Lee, K.; Phiri, I.; Kim, S.; Oh, K.; Ko, J. Preparation and Electrical Properties of Silicone Composite Films Based on Silver Nanoparticle Decorated Multi-Walled Carbon Nanotubes. *Materials* **2021**, *14*, 948. [[CrossRef](#)]
35. Shi, K.; Pang, X.; Zhitomirsky, I. Silver nanoparticle assembly on carbon nanotubes triggered by reductive surfactant coating. *Mater. Lett.* **2016**, *178*, 128–131. [[CrossRef](#)]
36. Lee, S.H.; Teng, C.C.; Ma, C.C.M.; Wang, I. Highly transparent and conductive thin films fabricated with nano-silver/double-walled carbon nanotube composites. *J. Colloid Interface Sci.* **2011**, *364*, 1–9. [[CrossRef](#)] [[PubMed](#)]
37. Ko, W.-Y.; Su, J.-W.; Guo, C.-H.; Fu, S.-J.; Hsu, C.-Y.; Lin, K.-J. Highly conductive, transparent flexible films based on open rings of multi-walled carbon nanotubes. *Thin Solid Films* **2011**, *519*, 7717–7722. [[CrossRef](#)]
38. Li, Y.-A.; Chen, Y.-J.; Tai, N.-H. Fast Process To Decorate Silver Nanoparticles on Carbon Nanomaterials for Preparing High-Performance Flexible Transparent Conductive Films. *Langmuir* **2013**, *29*, 8433–8439. [[CrossRef](#)] [[PubMed](#)]

Disclaimer/Publisher’s Note: The statements, opinions and data contained in all publications are solely those of the individual author(s) and contributor(s) and not of MDPI and/or the editor(s). MDPI and/or the editor(s) disclaim responsibility for any injury to people or property resulting from any ideas, methods, instructions or products referred to in the content.